Available free online at www.medjchem.com

Mediterranean Journal of Chemistry

Mediterranean Journal of Chemistry **2018**, 7(5), 359-369

Study of the Fe(II-III) hydroxysalts transformation according to the pH and the concentration of the ions present

Farida Termemil *, Marwa Ahmed-Malek, Assia Bourouba, and Mohamed-Rida Benloucif

Laboratoire de chimie des matériaux inorganiques, université Badji Mokhtar, BP 12 Sidi Amar, Annaba, Algérie

Abstract: Sulphated green rust, GR (SO_4^{2-}), is one of the main corrosion products of carbon steel in marine environments. It is Fe (II)-Fe(III) hydroxylsalt in sheets, consisting of alternating layers of iron-hydroxide type $Fe(OH)_2$, loaded positively due to the presence of the cations $Fe(III)$ and negative interlayers consisting of anions and water molecules. This compound is strongly associated with the metabolism of sulphate-reducing bacteria, and can also evolve under cathodic protection. Thus, recently, GR (CO_3^{2-}) has been detected in place of GR (SO_4^{2-}) on already corroded ordinary steel, newly subjected to cathodic protection. This presence is due to the pH and$[SO_4^{2-}]/[HCO_3^-]$ conditions imposed by the cathodic protection. In this paper, we chemically synthesize sulfated and carbonate green rust in a chlorinated medium; we then study their respective transformation according to the concentration $[SO_4^{2-}]$ / $[HCO_3^-]$ ratio and pH. Our results show that from a GR (SO_4^{2-}), GR (CO_3^{2-}) is formed from a pH ≥8.2 for $[SO_4^{2-}]$ / $[HCO_3^-]$ = 12 and without any change in pH for $[SO_4^{2-}]$ / $[HCO_3^-]$ <12. Whereas from GR (CO_3^{2-}), GR (SO_4^{2-}) is formed for $[SO_4^{2-}]$ / $[HCO_3^-]$ > 1 without any change in pH.

Keywords: steel; sea water; green rust; carbonate; sulfate; transformation.

Introduction

One of the main corrosion products of carbon steel in the marine environment is Fe(II-III) hydroxysulfate,

$Fe(II-III)$ ($Fe_4^{II}\,Fe_2^{III}(OH)_{12}SO_4.8H_2O$) [1,2], better known as sulphated green rust. Green rusts (GRs)are hydroxysalts of $Fe(II-III)$) in sheets, established by the alternation of layers of a hydroxide of type $Fe(OH)_2$, loaded positively due to the presence of the cations $Fe(III)$, and interlayers were established of anions and water molecules [3,1]. The thickness of the interlayer has been assumed to be defined by the intercalated anion. A compound containing spherical or planar anions, such as Cl^- or CO_3^{2-}, produce similar X-ray diffraction(XRD) patterns, and as a group, they have been known as GR1. The tetrahedral anions produce larger basal plane spacing: these have been known as GR2 [1,4,5]. There are various green rusts, in particular, those based on the main anions present in the sea water.

These are: Cl^-, SO_4^{2-} and HCO_3^-, so that it can form three types of GRs, the $GR(Cl^-)$, the $GR(SO_4^{2-})$ and, the $GR(CO_3^{2-})$.

In the conditions of concentration of the sea water in these various anions, $[SO_4^{2-}] = 0.02824 mol/l$; $[HCO_3^-] = 0.0023 mol/l$ and $[Cl^-] = 0.5368 mol/l$, only the sulphated variety is formed. To explain this peculiarity, experiments of a laboratory devoted to the oxidation by the air of a suspension of $Fe(OH)_2$ in the presence of $SO_4^{2-}$and Cl^- ions showed that the $GR(SO_4^{2-})$ formed instead of the $GR(Cl^-)$ even in solutions with large$[Cl^-]/[SO_4^{2-}]$ molar ratios [6].

Other experiments concerned this time the formation and the transformation of the $GR(Cl^-)$ from an aqueous suspension of $Fe(OH)_2$ in the presence of SO_4^{2-} and CO_3^{2-} ions. Both anions were separately added at the end of the formation of the $GR(Cl^-)$. In both cases, $GR(Cl^-)$ was transformed into $GR(SO_4^{2-})$ or into $GR(CO_3^{2-})$, this is explained by the fact that the layered structure of GRs presents a strong affinity for divalent anions [7].

The competition between the $SO_4^{2-}$and CO_3^{2-}ions have also been studied by the same authors.
In every case, the $GR(CO_3^{2-})$ of ($Fe_4^{II}Fe_2^{III}(OH)_{12}CO_3.2H_2O$) formula was obtained instead of the $GR(SO_4^{2-})$.

The $GR(SO_4^{2-})$ was obtained only when the CO_3^{2-}ion was insufficient to precipitate all Fe^{2+}ions present.

The green rust is an unstable compound and that is quickly oxidized into oxyhydroxide of Fe^{3+},(FeOOH) by the dissolved oxygen. So, at the beginning of the process of corrosion, the layer of rust

**Corresponding author : Farida Termemil*
Email address: mekkifarida@yahoo.fr
DOI: http://dx.doi.org/10.13171/mjc751912081134ft

Received October 2, 2018
Accepted November 6, 2018
Published December 8, 2018

formed on steel immersed in the sea water would consist of FeOOH near the electrolyte and $GR(SO_4^{2-})$ near the steel. However, after 6-12 months of exposure, $GR(SO_4^{2-})$ is consistently found to be associated with iron sulphide (FeS) and sulphate-reducing bacteria (BSR) [2].

The presence of iron sulphide (mackinawite, (FeS)) is a consequence of the metabolic activity of sulphate-reducing bacteria since sulfur is only present in seawater as sulphate [8]. SRBs are anaerobic microorganisms, and their presence among corrosion products confirms that anoxic conditions are established at the steel/$(GR(SO_4^{2-}))$ interface and inside the rust layer [9].

The anoxic conditions are because the dissolved oxygen is consumed outside of the layer of rust by the aerobic microorganisms and by the $GR(SO_4^{2-})$. This leads mainly to FeOOH.Thus, after some time, the kinetics of corrosion is no longer controlled by the transport of oxygen as this corrosion process is related to the activity of the microorganisms. Some authors suggest that the availability and transport of nutrients could be a limiting step [10].

A recent study [11] has shown that SRBs can reduce sulphate ions from the $GR(SO_4^{2-})$ structure. This phenomenon leads to the transformation of the $GR(SO_4^{2-})$ to a variety of compounds including iron sulphide (mackinawite).

Cathodic protection is widely used to protect submerged carbon steel structures against corrosion [12]. In the range of applied potentials, the reduction of dissolved oxygen is done at the interface of the metal and is accompanied, for more cathodic potentials, by the formation of hydrogen [13,14]. These two reactions produce OH^-hydroxyl ions which alkalinize the medium locally.

$$O_2 + 2H_2O + 4é \rightarrow 4OH^- \quad (1)$$
$$2H_2O + 2é \rightarrow H_2 + 2OH^- \quad (2)$$

This alkalinization of the medium leads to the change of the equilibrium of the inorganic carbon at the interface of the steel by promoting the formation of the carbonate ions (CO_3^{2-}) at the expense of the bicarbonate ions (HCO_3^-), according to the reaction (3). This leads also to the precipitation of $CaCO_3$ [13-15].

$$HCO_3^- + OH^- \rightarrow CO_3^{2-} + H_2O \quad (3)$$

The composition of the rust layers present on the surface of steel coupons immersed for 6 years and unprotected is similar to that of rust layers present under the calcareous deposits on protected and immersed coupons. These rust layers consist mainly of $GR(SO_4^{2-})$, magnetite, mackinawite, and Fe(III) oxyhydroxide. The same composition has been reported for immersed coupons for 6-12 months [8] and 11 years [6]. Recently, the analysis of the corrosion products present on coupons subjected to cathodic protection during one year after 5 years of immersion without protection shows that it is not the $GR(SO_4^{2-})$ that is present among the products of corrosion but the $GR(CO_3^{2-})$ [15]. These authors assume that the presence of this compound is due to the transformation of the $GR(SO_4^{2-})$ into $GR(CO_3^{2-})$ according to the following reaction:

$$Fe_4^{II}Fe_2^{III}(OH)_{12}SO_4.8H_2O + HCO_3^- \rightarrow Fe_4^{II}Fe_2^{III}(OH)_{12}CO_3.2H_2O + 6H_2O + SO_4^{2-} + H^+ \quad (4)$$

The reaction (4) is, in fact, the sum of the reactions (3) +(5)

$$Fe_4^{II}Fe_2^{III}(OH)_{12}SO_4.8H_2O + CO_3^{2-} \rightarrow Fe_4^{II}Fe_2^{III}(OH)_{12}CO_3.2H_2O + 6H_2O + SO_4^{2-} \quad (5)$$

This transformation has the same origin as that leading to the formation of calcareous and occurs as the pH or the concentration of carbonate ions increases through reactions (1) or (2) due to cathodic protection. It involves anion exchange in the interlayer without dissolving the solid phase. The hydroxide layers are preserved while the interlayers are changed from GR2 to GR1 without the possibility of incorporation of an anion HCO_3^- [15, 16].

In this study, we will synthesize $GR(SO_4^{2-})$ and $GR(CO_3^{2-})$, and we will study their relative stability according to the pH and on the presence of the HCO_3^- and SO_4^{2-} anions, in particular, to the concentration ratios of the sea water

$$[SO_4^{2-}]/[HCO_3^-] = \frac{[0.0282]}{[0.0023]} = 12.$$

Experimental conditions

Synthesis of green rust

The hydroxysulfate and hydroxycarbonate of iron (II)-(III) respectively $GR(SO_4^{2-})$ and $GR(CO_3^{2-})$ can be synthesized by oxidation of a precipitate of ferrous hydroxide in aqueous solution [6,17,18]. The simplest method is to precipitate $Fe(OH)_2$ from sodium hydroxide (NaOH) solution and ferrous sulfate solution to obtain $GR(SO_4^{2-})$ [18], but it is much more difficult to prepare $GR(CO_3^{2-})$ from a ferrous carbonate since the latter is insoluble;in this case,$Fe(OH)_2$ is precipitated from the ferrous sulphate before adding sodium carbonate to obtain the $GR(CO_3^{2-})$ [19]. An alternative method of $GR(SO_4^{2-})$ preparation has been developed to simulate the formation conditions of $GR(SO_4^{2-})$ in the marine environment [6]. This experimental approach, which derives from the fact that GRs have a high affinity for divalent ions [20], consists of using ferrous

chloride($FeCl_2, 4H_2O$) to obtain $Fe(OH)_2$ and then adding ($Na_2SO_4, 10H_2O$) or ($Na_2CO_3, 10H_2O$) respectively, just after the precipitation to provide the SO_4^{2-} or CO_3^{2-}ions necessary for obtaining green rust respectively sulfated or carbonated. It is this last experimental approach that we use in this study. The concentrations used are:

$[FeCl_2, 4H_2O] = 0.12\ mol.L^{-1}$
$[NaOH] = 0.2\ mol.L^{-1}$
$[Na_2SO_4, 10H_2O] = 0.02\ mol.L^{-1}$
$[Na_2CO_3], 10H_2O] = 0.02\ mol.L^{-1}$

Obtaining green rust requires an excess of iron (II) [17], so that an initial ratio $[Fe^{2+}]/[OH^-]$ greater than or equal to 0.6 is suitable. In the case of this study, the$[Fe^{2+}]/[SO_4^{2-}]$ or $[Fe^{2+}]/[CO_3^{2-}]$ was set at 6, which allows incorporation into green rust of almost all of the sulphates or carbonates respectively, according to the following reactions, which describe the formation of green rust from $Fe(OH)_2$:

$$5Fe(OH)_2 + Fe^{2+} + SO_4^{2-} + \tfrac{1}{2}O_2 + 9H_2O \rightarrow Fe_4^{II}Fe_2^{III}(OH)_{12}SO_4.8H_2O \quad (6)$$

$$5Fe(OH)_2 + Fe^{2+} + CO_3^{2-} + \tfrac{1}{2}O_2 + 3H_2O \rightarrow Fe_4^{II}Fe_2^{III}(OH)_{12}CO_3.2H_2O \quad (7)$$

The synthesis of the GR is carried out in a beaker containing 200ml of an aqueous suspension of $Fe(OH)_2$ and dipping in a thermostatic bath at $(25 \pm 0.5)°C$. The solution is vigorously stirred with a magnetic bar (stirring speed= 700rpm), constantly, to allow aeration homogeneity. Two electrodes introduced into this solution: a platinum electrode, and a saturated calomel electrode, although the Eh, electrode potential, is referred to the standard hydrogen electrode, to follow over time the evolution of the electrode potential of the solution. The chemical compounds used are provided by (Aldrich) and have a minimum purity of 99%. Once the green rust has been obtained, an event indicated by a rapid variation of Eh [6,17,18] (Figure 1), the precipitate is rapidly treated to prevent its oxidation by the ambient air, then either filtered for characterization or placed in a tightly closed bottle and covered with parafilm for preservation.

Green rust treatments

Two series of experiments were carried out:

Series 1: In an aqueous medium of in $\left[SO_4^{2-}\right]/[HCO_3^-] = \frac{[0.0282]}{[0.0023]} = 12$,

1. $GR(SO_4^{2-})$ + base
2. $GR(CO_3^{2-})$ + acid

Series 2: $GR(SO_4^{2-})$ or $GR(CO_3^{2-})$ + different $[SO_4^{2-}]/[HCO_3^-]$ at different pH. After treatment, the GR is analyzed by infrared spectroscopy and X-ray diffraction.

Instrumentation and sample preparation

The diffractograms were made using a Bruker-AXS D8 Advance diffractometer, whose Cu Kα radiation has a wave length $\lambda = 0.15406$ nm, and used in Bragg-Brentano geometry $[\theta - 2\theta]$.The precipitates are first filtered using a vacuum pump on a filter paper and the paste obtained is then rapidly deposited on the sample holder and covered with glycerol in order to limit the oxidation during the analysis.

The spectroscopic analysis were carried out using a Nexus Fourier Transform Infrared Spectrometer equipped with the ATR Smart MIRacle accessory and a capsule allowing to work in a controlled atmosphere. The precipitate is first filtered and rinsed with water and then with ethanol before being placed on the crystal. There, it is dried by a flow of nitrogen through the capsule.

Results and Discussions

Synthesis of $GR(CO_3^{2-})$ and $GR(SO_4^{2-})$

The formation and oxidation curves of $GR(CO_3^{2-})$ or $GR(SO_4^{2-})$, representing the electrode potential as a function of time, are presented in (Figure1). They have three stages [19]: the first stage, A, ends at the point of inflexion noted t_F, where all the ferrous hydroxide is transformed into of $GR(CO_3^{2-})$ or $GR(SO_4^{2-})$.

During the 2nd stage, B, ending at the point of inflection noted t_O, the GR is oxidized to ferric oxyhydroxide,

$$Fe_4^{II}Fe_2^{III}(OH)_{12}SO_4.8H_2O + \tfrac{3}{2}O_2 \rightarrow 5Fe^{III}OOH + SO_4^{2-} + Fe^{2+} + \tfrac{13}{2}H_2O \quad (8)$$

The third stage C which extends from t_O to t_∞ corresponds to the oxidation of the ferrous ions remaining in solution.

$$3Fe^{2+} + \tfrac{3}{4}O_2 + \tfrac{1}{2}H_2O \rightarrow Fe^{III}OOH + \mathbf{2}Fe^{3+} \quad (9)$$

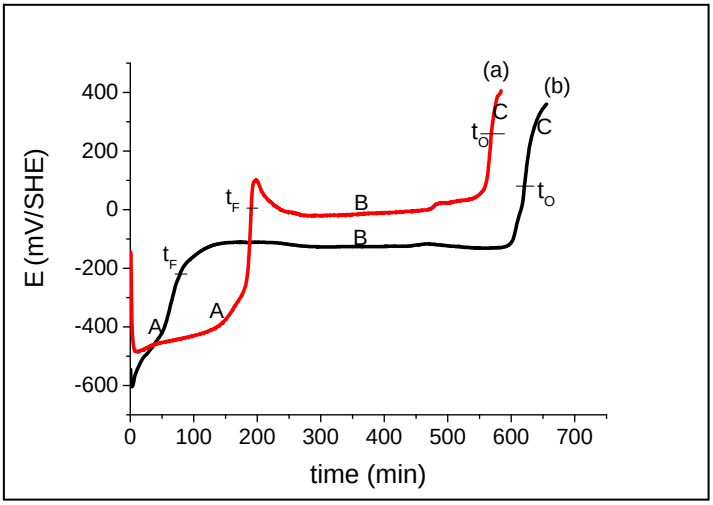

Figure 1. Typical E (mV/SHE) vs. time curve obtained during the oxidation by air of $Fe(OH)_2$ precipitated from: $FeCl_2, 4H_2O$ 0.12 mol. L^{-1} + NaOH 0.2 mol. L^{-1} and,
a): $Na_2SO_4, 10H_2O$ 0.02 mol. L^{-1}
b): $Na_2CO_3, 10H_2O$ 0.02 mol. L^{-1}

At point t_F where the conversion of $Fe(OH)_2$ to GR is complete, the reaction is stopped and the resulting GR is collected. (Figures 2a,b) show the typical absorption spectroscopic spectra respectively of $GR(CO_3^{2-})$ [16,21-23] and $GR(SO_4^{2-})$ [23,24] and their mixture in equal parts.

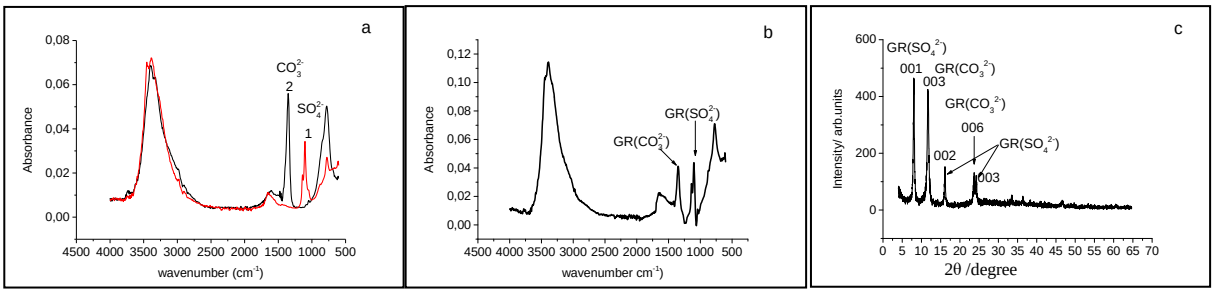

Figures 2. a) FTIR spectra analysis of : (1) $GR(SO_4^{2-})$, (2) $GR(CO_3^{2-})$ obtained during the oxidation by air of $Fe(OH)_2$precipitated from : $FeCl_2, 4H_2O$ 0.12 mol. L^{-1} + NaOH 0.2 mol. L^{-1} and:
1) $Na_2SO_4, 10H_2O$ 0.02 mol. L^{-1}, 2) $Na_2CO_3, 10H_2O$ 0.02 mol. L^{-1}; and taken at the time t_F in (Figure 1).
b) FTIR spectra analysis of a 50/50 mixture of $GR(SO_4^{2-})$ and $GR(CO_3^{2-})$.
c) XRD analysis of a 50/50 mixture of $GR(SO_4^{2-})$ and $GR(CO_3^{2-})$.

In (Figure 2a), the $GR(CO_3^{2-})$ and $GR(SO_4^{2-})$ spectra are superimposed. Each has a wide absorption band between $3300cm^{-1}$ and $3500cm^{-1}$, which is associated with stretching vibrations and the hydrogen bonding of water, and an absorption band at $1650cm^{-1}$ which is attributed to the water vibration of deformation. On the spectrum (1) the band at $1350cm^{-1}$ is attributed to the symmetric stretching mode of CO_3^{2-} [17].

On the spectrum (2), the band at $1100cm^{-1}$, supported by an another one at $1140cm^{-1}$, corresponds to the symmetric stretching mode of SO_4^{2-} [16,24]. Finally, the absorption bands at $779cm^{-1}$ and $840cm^{-1}$ are attributed to the deformation of $Fe-OH$ (crystal lattice vibration) and are the signature of green rust [16].

The (Figure 2c) shows the X-ray diffractogram of the mixture of equal parts of the two sulfated and carbonated GRs. It presents the three main intense line located at $2\theta \sim 8°; 16°$ and $24°$of $GR(SO_4^{2-})$,as well as the two main intense rays located at $2\theta \sim 12°$ and $23.6°$of $GR(CO_3^{2-})$ [8,15].

We also synthesized a suspension of $GR(CO_3^{2-})$ under the same conditions as the previous one, but from a mixture of the three anions to confirm the formation of the $GR(CO_3^{2-})$ at the expense of those based on the present anions. (Figures 3a,b) respectively show the evolution of the potential E of the electrode as a function of time during the formation and oxidation of the $GR(CO_3^{2-})$, and the X-ray diffractogram obtained during the analysis of the product collected at time tg. The diffractogram is typical of a $GR(CO_3^{2-})$ whose two main intense lines

are localized at $2\theta = 11.8°$ and $23.7°$ [8,15]. These results will serve as a reference to identify the transformation of $GR(SO_4^{2-})$ into $GR(CO_3^{2-})$ and vice versa in subsequent treatments.

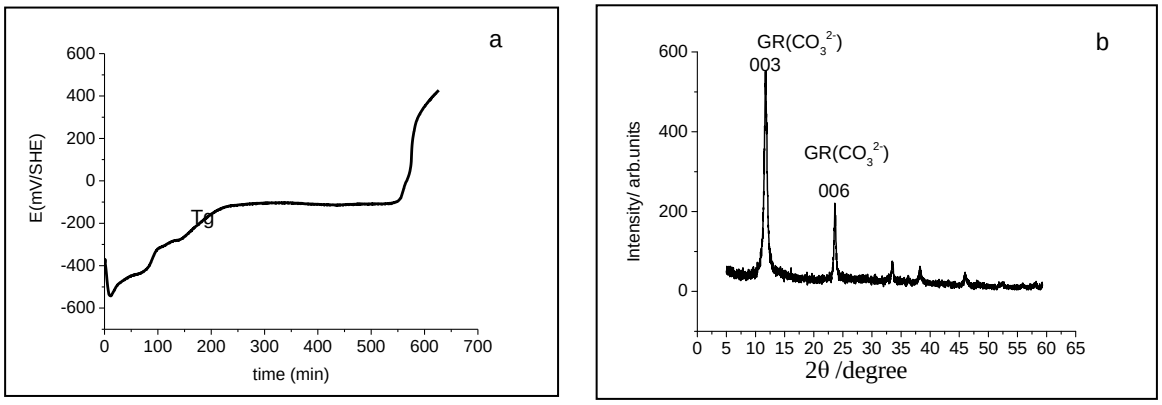

Figure 3. a) Typical E (mV/SHE) vs. time curve obtained during the oxidation by air of $Fe(OH)_2$ precipitated from:

$FeCl_2, 4H_2O$ 0.12 mol. L^{-1} + NaOH 0.2 mol. L^{-1} + Na_2SO_4 0.02 mol. L^{-1} + Na_2CO_3 0.02 mol. L^{-1}

T (25 ± 0.5) °C

b) XRD analysis of the $GR(CO_3^{2-})$ taken at time t_F.

$GR(SO_4^{2-})$ treatments

- **pH variation**

The $GR(SO_4^{2-})$ suspension obtained previously has an average pH of 7.2. To this suspension and with magnetic stirring, 0.0282 mol. L^{-1} of Na_2SO_4 and 0.0023 mol. L^{-1} of $NaHCO_3$ ($[SO_4^{2-}]/[HCO_3^-] = 12$) are added. The pH increases by about 3/10 of the unit and becomes equal on average to 7.53. NaOH is then added gradually to obtain suspensions at well-defined pH. Table 1 summarizes the results obtained.

Table 1. Treatment of $GR(SO_4^{2-})$ with: $[Na_2SO_4] = 0.0282$ mol. L^{-1} + $[NaHCO_3] = 0.0023$mo. L^{-1} ($[SO_4^{2-}]/[HCO_3^-] = 12$) pH variation by addition of OH^-.

$[GR(SO_4^{2-})] = 0.02$ mol. L^{-1}	$[SO_4^{2-}]/[HCO_3^-] = 12$						
pH adjusted	Without addition of OH^- 7.6	8.2	8.33	8.65	8.90	9.27	10.36
FTIR t = 0	$GR(SO_4^{2-})$	$GR(SO_4^{2-})$	$GR(SO_4^{2-})$ + $GR(CO_3^{2-})$	$GR(SO_4^{2-})$ + $GR(CO_3^{2-})$	$GR(SO_4^{2-})$ + $GR(CO_3^{2-})$	$GR(SO_4^{2-})$ + $GR(CO_3^{2-})$	$GR(SO_4^{2-})$ + $GR(CO_3^{2-})$
XRD t = 0	$GR(SO_4^{2-})$	$GR(SO_4^{2-})$	$GR(SO_4^{2-})$ + $GR(CO_3^{2-})$	$GR(SO_4^{2-})$ + $GR(CO_3^{2-})$	$GR(SO_4^{2-})$ + $GR(CO_3^{2-})$	$GR(SO_4^{2-})$ + $GR(CO_3^{2-})$	$GR(SO_4^{2-})$ + $GR(CO_3^{2-})$

At pH ≤ 8.2, we do not obtain $GR(CO_3^{2-})$, the FTIR spectroscopy analysis of the samples at pH = 7.6 and 8.2, respectively without and with pH modification, has a spectrum identical to that of the $GR(SO_4^{2-})$, as shown in the spectrum1of (Figure 2a).The X-ray diffraction analysis of these samples reveals the same GR compound and its spectrum is identical to the X-ray diffraction pattern of a $GR(SO_4^{2-})$ alone as shown at the (Figure 4a) [22].

From a pH = 8.33 we observe on the usual FTIR spectrum of the $GR(SO_4^{2-})$ a small absorption at $1350 cm^{-1}$ corresponding to the absorption wave number of the CO_3^{2-}group of the $GR(CO_3^{2-})$ (Figure 4b). This absorption is not due to a CO_3^{2-} ion adsorbed but to a CO_3^{2-} that is well incorporated in a green rust structure.

This phenomenon is observed because, at a pH = 8.90 and more, the shape of the peak is precise, the absorption is important, indicating the formation of a larger quantity of $GR(CO_3^{2-})$.

It should be noted, however, that the pH change must be progressive to prevent the dissolution of the precipitate. At $pH = 10.36$, the absorption is not greater than at $pH = 9.27$. The transformation of $GR(SO_4^{2-})$ into $GR(CO_3^{2-})$ is depending on the pH, but quantitatively it is not very important because $[HCO_3^-]$ is very small ($0.0023\ mol.l^{-1}$). For a given pH, if the transformation is complete, a maximum of $0.0023\ mol.l^{-1}$ of $GR(CO_3^{2-})$ would be formed and the ratio between the two GRs concentrations is about 8 in favor of $GR(SO_4^{2-})$. Furthermore, after 14 days of aging, the pH of the sample was found to have decreased slightly from its earlier value of 8.2 [8.18], and its FTIR spectrum reveals a small absorption indicating the formation of a $GR(CO_3^{2-})$ (Figure 4c). The transformation does not necessarily occur in real time even at pH > 8.40. Thus the compound was detectable half a day later. The (Figures 4 c,d) respectively show FTIR and X-ray diffraction spectra of a sample which has a pH of 8.65 and which revealed the presence of $GR(CO_3^{2-})$ only after 24h of aging. From these results, it can be assumed that the transformation of $GR(SO_4^{2-})$ into $GR(CO_3^{2-})$ is possible at pH close to 8.2.

We also noticed during these tests, that the pH decreases during aging. If it reaches a value of less than about 8, the $GR(CO_3^{2-})$ formed by transformation after alkalinization treatment disappears. It seems that the $GR(CO_3^{2-})$ compound is unstable at $pH \leq 8$ in a sulphated environment and that the opposite reaction would be possible. According to reaction (4) a drop in pH causes the reaction to shift in the direction of $GR(SO_4^{2-})$ formation.

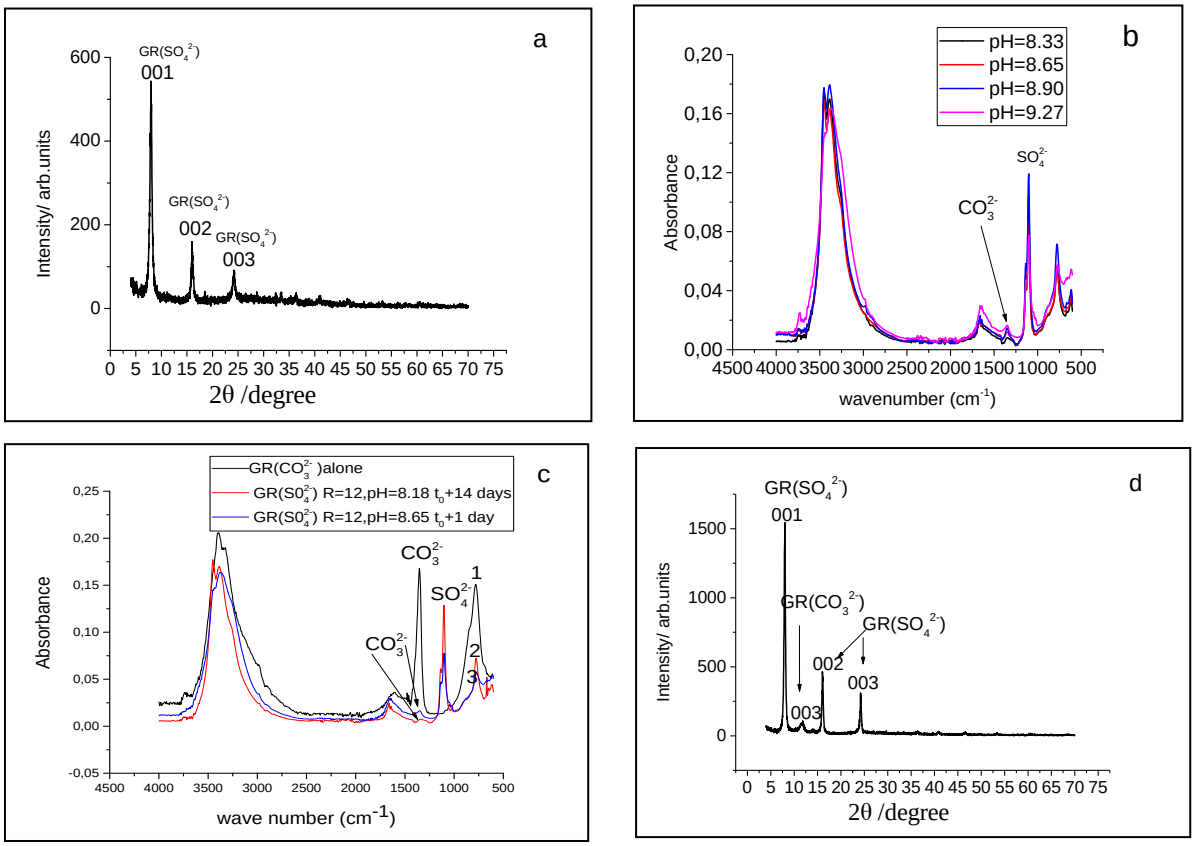

Figures 4. a) XRD of analysis of the $GR(SO_4^{2-})$, $R = 12$ at $pH = 8$ and $t = 0$ min.
b) FTIR spectra of analysis of $GR(SO_4^{2-})$, $R = 12$ at $\neq pH$
c) FTIR spectra of analysis of
1) $GR(CO_3^{2-})$ alone
2) $GR(SO_4^{2-})$, R=12, pH=8.18, after 14days of aging
3) $GR(SO_4^{2-})$, R=12, pH=8.65, after 1day of aging
d) XRD of analysis of $GR(SO_4^{2-})$, $R = 12$ at $pH = 8.65$ and $t_0 + 1day$

- **Variation of the $[SO_4^{2-}]/[HCO_3^-]$ ratio**

To the suspension of $GR(SO_4^{2-})$ obtained previously and with magnetic stirring, $0.0282\ mol.L^{-1}$ of $[Na_2SO_4]$ is added. Afterwards, sodium bicarbonate, $NaHCO_3$, is added progressively to vary the $[SO_4^{2-}]/[HCO_3^-]$ ratio from value 12 to 0.5.

The variation of the ratio $[SO_4^{2-}]/[HCO_3^-]$ ratio by increasing the $[HCO_3^-]$ from an initial concentration of $0.0023\ mol.L^{-1}$, lead to a shift of the reaction

towards the formation of $GR(CO_3^{2-})$ by an exchange of anions, as shown in the reaction (4) [15].

For a ratio of $[SO_4^{2-}]/[HCO_3^-] = 12$, we saw that the $GR(SO_4^{2-})$ did not convert to $GR(CO_3^{2-})$ if the pH is not increased by 8.2, therefore this reaction would be possible only by the consumption of H^+ ions. For $R < 12$, the amount of $NaHCO_3$ to be added is calculated relatively to $[SO_4^{2-}] = 0.0282\ mol.L^{-1}$ which remains constant. The $[SO_4^{2-}]/[HCO_3^-]$ ratios considered are as follows:

Table 2. Treatment of $GR(SO_4^{2-})$ with $[Na_2SO_4] = 0.0282\ mol.L^{-1} + [NaHCO_3]$ variable.

$[GR(SO_4^{2-})] = 0.02\ mol.L^{-1}$	$[SO_4^{2-}]/[HCO_3^-] = R$			
R	12	6	1	0,5
$+ [Na_2SO_4] mol.L^{-1}$	0.0282	0.0282	0.0282	0.0282
$+ [NaHCO_3] mol.L^{-1}$	0.0023	0.0046	0.0282	0.0565
pH	7.69	7.74	7.75	7.77
FTIR t_0	$GR(SO_4^{2-})$	$GR(SO_4^{2-})$ + $GR(CO_3^{2-})$	$GR(SO_4^{2-})$ + $GR(CO_3^{2-})$	$GR(SO_4^{2-})$ + $GR(CO_3^{2-})$

Indeed, if the concentration of $[HCO_3^-]$ ion increases this means that for a concentration ratio of $[SO_4^{2-}]/[HCO_3^-] \leq 6$, there is the formation of $GR(CO_3^{2-})$ from a $GR(SO_4^{2-})$ (Figure 5).Thus, the transformation of $GR(SO_4^{2-})$ into $GR(CO_3^{2-})$ in the presence of $SO_4^{2-}$and HCO_3^- ions seem to depend on the value of the concentration ratio of the two species of anions [23] for a $pH < 8.2$ in our operating conditions. For a ratio of concentration equal to or less than unity, so an amount of $NaHCO_3$ bigger than that of SO_4^{2-} involved in the structure of $GR(SO_4^{2-})$, the transformation of $GR(SO_4^{2-})$ to $GR(CO_3^{2-})$ is not complete since the analysis of the sample reveals the presence of the two GRs after a week of aging. For an initial formation with an equal concentration of anions, that is to say, for a ratio equal to 1, it is only the $GR(CO_3^{2-})$ which is formed [1].

The (Figure 3b) shows the X-ray diffractogram of a $GR(CO_3^{2-})$ compound prepared under these conditions. In a recent study [23], $GR(CO_3^{2-})$ was formed from a solution containing sulphate and bicarbonate ions in a ratio $[SO_4^{2-}]/[HCO_3^-] = 12$ and a low concentration of bicarbonate ions ($0.003\ mol.L^{-1}$). For the same concentration ($[HCO_3^-] = 0.003\ mol.L^{-1}$), an electro-generated $GR(CO_3^{2-})$ formation, meaning from carbon steel with anodic polarization, was obtained in the sulfated medium in a concentration ratio($[SO_4^{2-}]/[HCO_3^-]$) equal to 10 [8].In this case, the amount of $GR(CO_3^{2-})$ formed is very small. Keeping the same ratio and multiplying$[SO_4^{2-}]$ and $[HCO_3^-]$ by**10**, the amount of green rust formed remains in favor of $GR(SO_4^{2-})$.

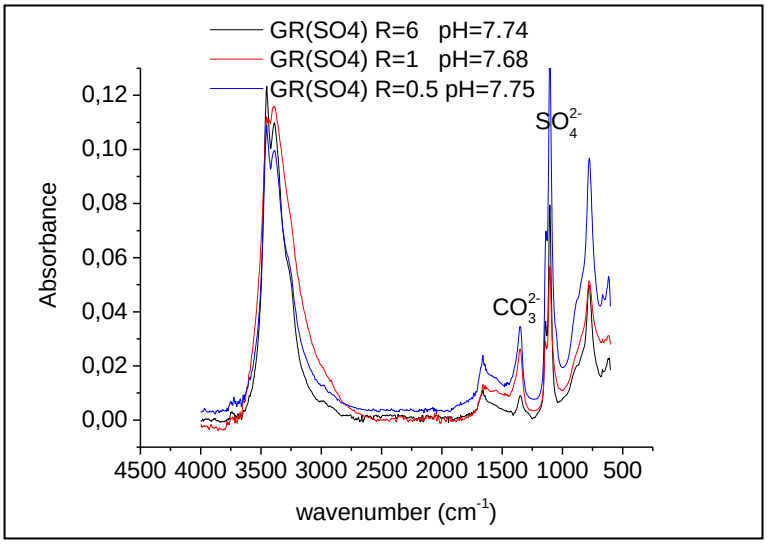

Figure 5. FTIR spectra of analysis of $GR(SO_4^{2-})$ at R variable and without pH modification

$GR(CO_3^{2-})$ treatments

- **pH Variation**

➢ $GR(CO_3^{2-})$alone

To the suspension of $GR(CO_3^{2-})$ obtained previously and with magnetic stirring, H^+ions are added to lower its pH gradually. Samples are taken and analyzed at given pH.

➢ $GR(CO_3^{2-})$+$[SO_4^{2-}]$ +$[HCO_3^-]$

To the suspension of $GR(CO_3^{2-})$ obtained previously and with magnetic stirring, we add $0.0282\ mol.L^{-1}\ Na_2SO_4$ + $0.0023 mol.L^{-1} NaHCO_3$, ($[SO_4^{2-}]/[HCO_3^-] = 12$) and gradually HCl to obtain solutions with a well-defined pH. Table 3 regroups the results of these two tests.

Table 3. Treatment of $GR(CO_3^{2-})$ with $[Na_2SO_4] = 0.0282\ mol.L^{-1}$ + $[NaHCO_3] = 0.0023 mol.L^{-1}$ ($[SO_4^{2-}]/[HCO_3^-] = 12$) , pH variation by addition of H^+.

$[GR(CO_3^{2-})] = 0.02\ mol.L^{-1}$	without addition of Na_2SO_4+$NaHCO_3$				$+[SO_4^{2-}]/[HCO_3^-] = 12$		
pH adjusted	7.26	7.10	6.90	6.80	7.10	6.90	6.80
FTIR t=0	$GR(CO_3^{2-})$	$GR(CO_3^{2-})$	$GR(CO_3^{2-})$	No GR	$GR(CO_3^{2-})$ + $GR(SO_4^{2-})$	No GR	No GR
XRD t_0 + 1day	$GR(CO_3^{2-})$	$GR(CO_3^{2-})$	$GR(CO_3^{2-})$	No GR	$GR(CO_3^{2-})$ + $GR(SO_4^{2-})$	$GR(CO_3^{2-})$ + $GR(SO_4^{2-})$	No GR
FTIR t+8days	$GR(CO_3^{2-})$	$GR(CO_3^{2-})$	No GR	No GR	$GR(CO_3^{2-})$ + $GR(SO_4^{2-})$	$GR(CO_3^{2-})$ + $GR(SO_4^{2-})$	No GR

The $GR(CO_3^{2-})$ suspension prepared has an average pH of 7.70. This increases by one to two-tenths of a unit (1/10 to 2/10) after the addition of sodium sulphate and sodium bicarbonate. The pH is then adjusted to values close to neutrality to allow the $GR(CO_3^{2-})$ to transform itself or not into $GR(SO_4^{2-})$. The $GR(CO_3^{2-})$ alone, treated with HCl, is stable to pH = 6.90. At pH = 6.80, it has been dissolved under the effect of H^+ ions and we do not observe GR on the infrared spectrum.

The $GR(CO_3^{2-})$ sample in the presence of SO_4^{2-} and HCO_3^- ions and treated with H^+did not reveal any GR compound at pH = 6.90; this same sample analyzed 24 hours later revealed the presence of the two GRs, the $GR(CO_3^{2-})$ and the $GR(SO_4^{2-})$, (Figure 6). The GRs have probably dissolved and reformed during aging. Note that the main ($2\theta = 8°$) line of the $GR(SO_4^{2-})$, is as important as that the $GR(CO_3^{2-})$; ($2\theta = 11.7°$). These results also show that $GR(CO_3^{2-})$is not stable at pH < 6.90 in an environment with or without SO_4^{2-} ions.

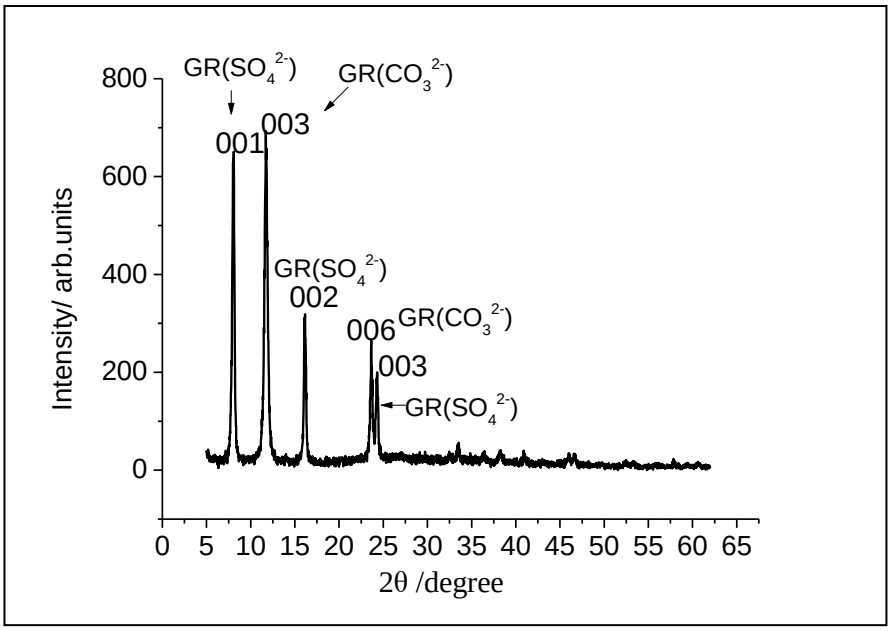

Figure 6. XRD of analysis of $GR(CO_3^{2-})$ with R = 12 at pH = 6.90, and at t_0 + 1day.

- **Variation of the $[SO_4^{2-}]/[HCO_3^-]$ ratio**

In this part, we did two types of tests: in the first test we treat the $GR(CO_3^{2-})$ with SO_4^{2-} and HCO_3^- ions in a variable ratio ranging from 12 to 0.5 ; while in the second test, we adjusted the pH to 8.28 to recall the physicochemical conditions of the sea water; Table 4 summarizes the results obtained :

Table 4. Treatment of $GR(CO_3^{2-})$ with $[Na_2SO_4] = 0.028\ mol.L^{-1} + [NaHCO_3]$ variable.

$GR(CO_3^{2-}) = 0.02\ mol.L^{-1}$	$[SO_4^{2-}]/[HCO_3^-] = R$								
R	12	6	1	0,5		12	6	1	0.5
pH	7.72	7.81	7.83	7.83		8.22	8.20	8.21	8.28
+ $[Na_2SO_4]mol.L^{-1}$	0.0282	0.0282	0.0282	0.0282		0.0282	0.0282	0.0282	0.0282
+ $[NaHCO_3]mol.L^{-1}$	0.0023	0.0046	0.0282	0.0565		0.0023	0.0046	0.0282	0.0565
FTIR t_0	$GR(SO_4^{2-})$ + $GR(CO_3^{2-})$	$GR(SO_4^{2-})$ + $GR(CO_3^{2-})$	$GR(CO_3^{2-})$	$GR(CO_3^{2-})$		$GR(CO_3^{2-})$ + $GR(SO_4^{2-})$	$GR(CO_3^{2-})$ + $GR(SO_4^{2-})$	$GR(CO_3^{2-})$	$GR(CO_3^{2-})$

The results show that, for the concentration ratios considered, the $GR(CO_3^{2-})$ is transformed into $GR(SO_4^{2-})$ when it is in an environment where the concentration in its anion is 6 to 12 times lower than that of the sulfate ion($[HCO_3^-] < 6[SO_4^{2-}]$), this ratio would be less than 4 according to [25], so $GR(SO_4^{2-})$ is not found when R is 1 and 0.5. (Figure 7a) shows the infrared spectra of the GRs obtained at different R. The absorption due to $GR(SO_4^{2-})$ decreases when R decreases. For $R = 12$ the sample was analyzed a second time 24h after the treatment, its diffractogram, shown in (Figure 7b), is that of a mixture of the two GRs, where the intensity of the main line of the $GR(SO_4^{2-})$is ¼ of that of the $GR(CO_3^{2-})$. This shows that the transformation of the $GR(CO_3^{2-})$ into $GR(SO_4^{2-})$ is only partial!

For $R = 1$ the sample was analyzed after one week of aging, its X-ray diffractogram presented in (Figure 7c) is that of a $GR(CO_3^{2-})$ alone. Samples adjusted to $pH = 8.2$ gave similar results to those whose pH was unchanged. These results show that the transformation of the $GR(CO_3^{2-})$ in to $GR(SO_4^{2-})$ for this ratio do not depend on the pH of the solution. In general, $GR(CO_3^{2-})$ is formed by alkalinization of a $GR(SO_4^{2-})$ from $pH = 8.2$ if $R = 12$, and without pH change for $R \leq 6$.

The $GR(SO_4^{2-})$ is formed from a $GR(CO_3^{2-})$ for $R \geq 6$ whatever the pH (under our test conditions: $7.7 \leq pH \leq 8.2$).

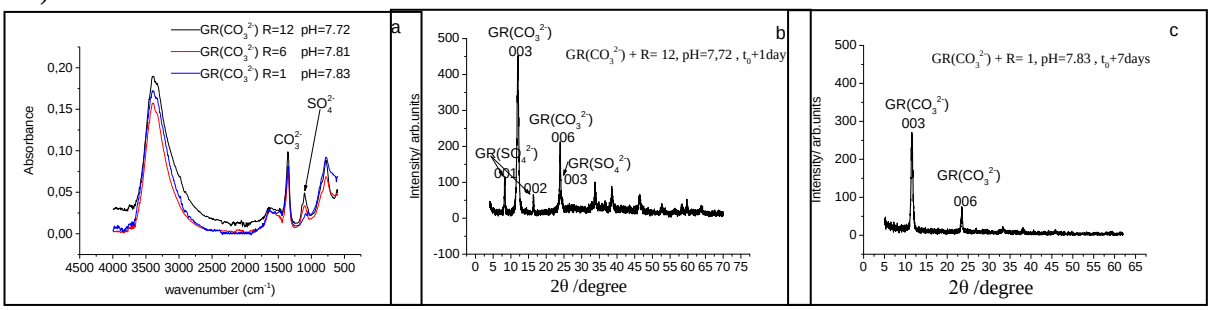

Figure 7. a) FTIR spectra of $GR(CO_3^{2-})$, R variable without pH modification
b)XRD of analysis of $GR(CO_3^{2-})$, $R = 12$ at $pH = 7.72$ and at $t_0 + 1day$
c) XRD of analysis of $GR(CO_3^{2-})$, $R = 1$ at $pH = 7.83$ and at $t_0 + 7days$

Conclusion

The transformation of the $GR(SO_4^{2-})$ into $GR(CO_3^{2-})$ is characterized by an exchange of the SO_4^{2-} ion engaged in a green rust structure and the free CO_3^{2-}anion in solution. This exchange is related to the value of the concentration of the sulphate to bicarbonate species ratios which are present and to a lesser extent to the pH of the medium. For a $[0.0282]/[0.0023] = 12$ which is that of seawater, the transformation of $GR(SO_4^{2-})$ into $GR(CO_3^{2-})$ is related to the pH of the solution. For ratios of concentrations lower than 12, the transformation from $GR(SO_4^{2-})$ to $GR(CO_3^{2-})$ no longer depends on pH and becomes dependent only on the value of this ratio. We have seen that the inverse transformation, from $GR(CO_3^{2-})$ to $GR(SO_4^{2-})$ is also possible, but only for $R \geq 6$. A drop in pH would favor this

transformation; thus, for $R = 12$, the transformation is greater at $pH = 6.90$ than at $pH = 7.72$!. Whatever the initial green rust, the transformation is only partial for all the pH and concentration ratios considered in this study.

Acknowledgements

The authors thank the laboratory LASIE of the University of La Rochelle for its help in the characterization of their samples.

References

1- L. Simon, M. François, P. Refait, G. Renaudin, M. Lelaurin, J.M.R. Génin, Structure of the Fe(II-III) Layered double hydroxysulphate green rust two from Rietveld analysis, Solid Stat. Sci, **2003**, 5, 327–334.

2- S. Pineau, L. Quillet, M. Jannin, Ch. Caplat, I. Dupont-Morral, Ph. Refait, Formation of the Fe(II–III) hydroxysulphate green rust during marine corrosion of steel associated to molecular detection of dissimilatory sulphite-reductase, Corros. Sci., **2008,** 50**,** 1099–1111.

3- Ph. Refait, M. Abdelmoula, J.M.R. Génin, Mechanisms of formation and structure of green rust one in aqueous corrosion of iron in the presence of chloride ions, Corros. Sci., **1998,** 40,1547–1560.

4- B.C. Christiansen, T. Balic-Zunic, P.O. Petit, C. Frandsen, S. Mørup, H. Geckeis, A. Katerinopoulou, S.L. Svane Stipp, Composition and structure of an Iron bearing, Layered Double Hydroxide (LDH) – Green Rust Sodium Sulphate, Geochimica et Cosmochimica Acta, **2009**, 73, 3579–3592.

5- S. J. Mills, A.G. Christy, J.M.R. Genin, T. Kameda and F. Colombo, Nomenclature of the hydrotalcite supergroup: natural layered double hydroxides, Mineralogical Magazine, **2012**, 76, 1289–1336.

6- Ph. Refait, J.B. Memet, C. Bon, R. Sabot, J.M.R. Génin, Formation of the Fe(II)–Fe(III), Hydroxysulphate green rust during marine corrosion of steel, Corros.Sci., **2003**, 45, 833–845.

7- Ph. Refait, S.H. Drissi, J. Pytkiewicz, J.M.R. Génin, The anionic species competition in aqueous iron corrosion: Role of various green rust compounds, Corros. Sci., **1997,** 39, 1699–1710.

8- Ph. Refait, D.D. Nguyen, M. Jeannin, S. Sable, M. Langumier, R. Sabot, Electrochemical Formation of Green Rusts in Deaerated Seawater-Like Solutions, Electrochimica Acta, **2011**,56, 6481–6488.

9- Ph. Refait, A.M. Grolleau, M. Jeannin, E. François, R. Sabot, Corrosion of Mild Steel at The seawater/sediments interface: mechanisms and kinetics, Corros. Sci., 2018**,** 130, 76–84.

10- R.E. Melchers, T. Wells, Models for The Anaerobic Phases of Marine Immersion Corrosion. Corros. Sci., **2006**, 48, 1791–1811.

11- M. Langumier, R. Sabot, R. Obame-Ndong, M. Jeannin, S. Sablé, Ph. Refait, Formation of Fe(III)-containing mackinawite from hydroxysulphate green rust by sulphate reducing bacteria, Corros. Sci., **2009,** 51, 2694–2702.

12- Y.-S. Kim, S.K. Lee, H.J. Chung, J.G. Kim, Influence of a simulated deep sea condition on the cathodic protection and electric field of an underwater vehicle, Ocean Engineering, **2018**, 148, 223–233.

13- Ph. Refait, M. Jeannin, R. Sabot, H. Antony, S. Pineau, Corrosion and cathodic protection of carbon steel in the tidal zone: products, mechanisms and kinetics, Corros. Sci., **2015**, 90, 375–382.

14- D. Nguyen Dang, L. Lanarde, M. Jeannin, R. Sabot, Ph. Refait, Influence of soil moisture on the residual corrosion rates of buried carbon steel structures under cathodic protection, Electrochimica Acta, **2015**, 176, 1410–1419.

15- Ph. Refait, M. Jeannin, R. Sabot, H. Antony, S. Pineau, Electrochemical formation and transformation of corrosion products on carbon steel under cathodic protection in seawater, Corros. Sci., **2013**,71, 32–36.

16- L. Legrand, G. Sagon, S. Lecomte, A. Chausse, A Raman and Infrared Study of a new carbonate green rust obtained by the electrochemical way, Corros. Sci., **2001**, 43, 1739–1749.

17- A.A. Olowe, J.M.R. Génin, The mechanism of oxidation of ferrous hydroxide in sulphated aqueous media: Importance of the initial ratio of the reactants, Corros. Sci., **1991**, 32, 965–984.

18- J.M.R. Génin, A.A. Olowe, P. Refait, L. Simon, On the stoichiometry and pourbaix diagram of Fe(II)-Fe(III) hydroxy-sulphate or sulphate containing green rust 2: An electrochemical and Mossbauer spectroscopy study, Corros. Sci., **1996**, 38, 1751–1762.

19- S.H. Drissi, Ph. Refait, M. Abdelmoula and J.M.R. Génin, The preparation and thermodynamic properties of Fe(II)-Fe(III) hydroxide-carbonate (Green Rust 1): Pourbaix diagram of iron in carbonate-containing aqueous media, Corros. Sci., **1995**, 37, 2025–2041.

20- S. Miyata. Anion-Exchange Properties of Hydrotalcite-Like Compounds, Clays Clay Miner., **1983**, 31, 305–311.

21- L. Legrand, L. Mazerolles, A. Chaussé, The Oxidation of Carbonate Green Rust into Ferric Phases: Solid-State Reaction or Transformation Via Solution, Geochimica et Cosmochimica Acta, **2004**, 68, 3497–3507.

22- R. Guilbaud, M. L. White, S.W. Poulton, Surface charge and growth of sulphate and carbonate green rust in aqueous media, Geochimica et Cosmochimica Acta, **2013**, 108, 141–153.

23- Ph. Refait, J.A. Bourdoiseau, M. Jeannin, D.D. Nguyen, A. Romaine, R. Sabot, Electrochemical formation of carbonated corrosion products on carbon steel in deaerated solutions, Electrochimica Acta, **2012**, 79, 210–217.

24- W. Yin, L. Huang, E.B. Pedersen, C. Frandsen, H.C.B. Hansen, Glycine buffered synthesis of layered Iron(II)-Iron(III) Hydroxides (Green Rusts), Journal of Colloid and Interface Science, **2017**,497, 429–438

25- F. Termemil, M.R. Benloucif, A. Benmoussa, R. Chater, 7th African Conference on non-destructive Testing ACNDT 2016 and The 5th International Conference on Welding, Non-Destructive Testing Materials and Alloys Industry (IC-WNDT-MI'16), Oran, Algeria **2016** November 26–28.